Pharm Res (2010) 27:1914–1926
DOI 10.1007/s11095-010-0196-5

RESEARCH PAPER

# Paclitaxel-Loaded, Folic-Acid-Targeted and TAT-Peptide-Conjugated Polymeric Liposomes: *In Vitro* and *In Vivo* Evaluation

Peiqi Zhao • Hanjie Wang • Man Yu • Shuzhen Cao • Fei Zhang • Jin Chang • Ruifang Niu

Received: 3 April 2010 / Accepted: 15 June 2010 / Published online: 26 June 2010
© Springer Science+Business Media, LLC 2010

## ABSTRACT

***Objective*** Folic acid and TAT peptide were conjugated on the octadecyl-quaternized, lysine-modified chitosan-cholesterol polymeric liposomes (FA-TATp-PLs) to investigate their potential feasibility for tumor-targeted drug delivery.

***Methods*** FA-TATp-PLs encapsulating paclitaxel or calcein were synthesized and characterized. Cellular uptake of PLs, FA-PLs, TATp-PLs and FA-TATp-PLs was studied by confocal laser scanning microscopy (CLSM) in folate receptor (FR)-positive KB nasopharyngeal epidermal carcinoma cells and FR-deficient A549 lung cancer cells. *In vitro* and *in vivo* antitumor activity of paclitaxel-loaded FA-TATp-PLs were also evaluated in KB and A549 cells as well as in a murine KB xenograft model.

***Results*** Our data showed that 80% paclitaxel released from FA-TATp-PLs in 2 weeks. Different from other various PLs, CLSM analyses showed that FA-TATp-PLs had a significantly high efficient intracellular uptake in both KB and A549 cells. These data revealed the targeting effects of folate decoration, the transmembrane ability of TAT peptide as well as a synergistic interaction between them. In addition, paclitaxel-loaded FA-TATp-PLs exhibited a more superior antitumor effect *in vitro* and *in vivo* as compared to that with Taxol®.

***Conclusions*** FA-TATp-PLs possessing both targeting effect and transmembrane ability may serve as a promising carrier for the intracellular delivery of therapeutic agents.

**KEY WORDS** cellular uptake · paclitaxel · polymeric liposomes · target delivery

## ABBREVIATIONS

| | |
|---|---|
| DAPI | 4,6-Diamidino-2-phenylindole |
| DLS | dynamic light scattering |
| DMSO | dimethyl sulfoxide |
| DTT | dithiothreitol |
| ER | encapsulation rate |
| FA | folic acid |
| FR | folate receptor |
| HPLC | high performance liquid chromatography |
| LE | loading efficiency |
| MTT | 3-[4,5-dimethylthiazol-2-yl]-2,5-diphenltetrazolium bromide |
| MW | molecular weight |
| OQLCS | octadecyl-quaternized lysine modified chitosan |
| PBS | phosphate-buffered saline |
| PLs | Polymeric liposomes |
| PTX | paclitaxel |
| SD | standard deviation |
| SPDP | N-succinimidyl-3-(2-pyridyldithio) propionate |
| TATp | transactivating transcriptional activator peptide |
| TEM | transmission electron microscopy |

## INTRODUCTION

Paclitaxel (PTX), a commonly employed chemotherapeutic drug, promotes the assembly and stabilization of microtubules

P. Zhao • S. Cao • F. Zhang • R. Niu (✉)
The Key Laboratory of Breast Cancer Prevention and Therapy
Ministry of Education, Tianjin Medical University
Cancer Institute and Hospital
Tianjin 300060, China
e-mail: niurf1982@yahoo.com.cn

H. Wang • J. Chang (✉)
Institute of Nanobiotechnology, School of Materials Science
and Engineering, Tianjin University and Tianjin Key Laboratory
of Composites and Functional Materials
Tianjin 300072, China
e-mail: jinchang@tju.edu.cn

M. Yu
Center for Advanced Research in Environmental Genomics (CAREG)
Department of Biology and Department of Cellular and Molecular
Medicine, University of Ottawa
Ottawa, Ontario, Canada K1N 6N5

and interferes with essential cellular functions such as mitosis, cell transport, and cell motility (1–3). It is one of the most widely used anticancer drugs for the treatment of various human malignancies. Due to its poor solubility in water, PTX is currently formulated in a 1:1 mixture of Cremophor EL (a polyethoxylated castor oil) and ethanol to create Taxol®. However, Cremophr EL has been documented for various serious side effects, including acute hypersensitivity reactions, nephrotoxicity, neurotoxicity, and cardiotoxicity (4). Therefore, there is an urgent need to develop a biocompatible and efficacious PTX formulation that could have minimal side effects and promote specific uptake into tumor cells. Ideally, the drug should be selectively and efficiently enriched in the tumor lesions without damaging normal tissues. A number of functional drug carriers have been investigated, mainly including liposomes (5), micelles (6), polymeric biodegradable nanoparticles (7–9), dendrimers (10) and hydrogels (11–13).

Polymeric liposomes (PLs) have attracted much attention in drug delivery systems due to their high loading efficiency (LE), combined with a great surface area and an ease of surface modification. However, achieving a high degree of drug loading is only one of the major factors determining an efficient drug delivery. Refined targeting selectivity and high delivery efficiency are two equally important goals in the development of drug delivery systems (14–16).

One strategy to enhance tumor-specific targeting for PLs is active targeting. It can be achieved by conjugating targeting moiety onto the outer surface of the lipid bilayer of the liposome that specifically binds to receptors that are either uniquely expressed or overexpressed on the tumor cell surface, but have low or negligible expression in normal cells. Folic acid (FA) could selectively bind to folate receptor (FR), a 38 kDa glycosyl-phosphaidyl inositol-anchored cell surface receptor, which is significantly upregulated in ovary, lung, endometrium, brain, head and neck, kidney, breast, and myeloid cancers (17–19) as compared to that in normal tissues (20).

Using FA as targeting moiety, PLs can be selectively delivered to tumor cells overexpressing FR; however, efficient delivery of PLs still remains as a major problem, at least partially because cell membrane constitutes a major barrier for intracellular delivery of relatively large particles (21). Transactivating transcriptional activator peptide (TATp), as an effective transport carrier, possesses the ability to facilitate the efficient uptake of various cargos ranging from small peptide sequences to large biomolecules like liposomes and polymers (22–24). Nonetheless, the exact mechanism underlying TAT peptide-mediated intracellular delivery of small and large molecules remains obscure. Despite its unmatched ability to efficiently translocate cargo molecules into cells, TAT peptide does not possess targeting selectivity in cell entry, significantly hindering its potential clinical applications (25). Hence, it would be desirable to combine the specific targeting of FA ligands with the transmembrane ability of TAT peptide when designing a PLs-based drug delivery system.

As a novel chitosan derivative, octadecyl-quaternized lysine-modified chitosan (OQLCS) has a good solubility both in water and organic solvents and has an amino group to which functional groups such as FA and TAT peptide could be connected. Moreover, OQLCS is very cheap and can easily be reconstituted into liposomes. On the basis of OQLCS and cholesterol, we recently synthesized folic acid-modified and TAT peptide-conjugated PLs (FA-TATp-PLs) that possess all the above-mentioned functions. Here, we describe how PTX-loaded FA-TATp-PLs composed of PTX, FA-conjugated OQLCS, TAT peptide and cholesterol were synthesized (Fig. 1). Their various physicochemical properties, such as particle size, polydispersity, surface morphology, drug encapsulation efficiency and *in vitro* drug release profile, were investigated. To demonstrate the function of the targeting ability of FA ligand and transmembrane ability of TAT peptide, cellular uptake efficiency and toxicity of calcein or paclitaxel-loaded FA-TATp-PLs were evaluated in FR-positive KB nasopharyngeal epidermal carcinoma cells and FR-negative A549 lung cancer cells. *In vivo* antitumor activity of PTX-loaded FA-TATp-PLs was also examined in mice bearing nasopharyngeal carcinoma compared with Taxol®.

## MATERIALS AND METHODS

### Materials and Reagents

Chloroform, cholesterol, 4,6-Diamidino-2-phenylindole (DAPI), Sulfosuccinimidyl-[3′(2-pyridyldithio)-propionamido] hexanoate (Sulfo-LC-SPDP), dimethyl sulfoxide (DMSO), dithiothreitol (DTT), phosphate-buffered saline (PBS) and 3-[4,5-dimethylthiazol-2-yl]-2,5-diphenltetrazolium bromide (MTT) were purchased from Sigma-Aldrich (St. Louis, MO, USA). OQLCS and FA-OQLCS were synthesized in our laboratory as previously described in the literature (26). TAT peptide of the sequence Tyr-Gly-Arg-Lys-Lys-Arg-Arg–Gln-Arg-Arg-Arg (MW 1,560 Da) was synthesized by GL Biochem Ltd. (Shanghai, China). Taxol and paclitaxel were purchased from Sike Pharmaceutical Co., Ltd. (Jiangsu, China). Reagents for cell culture were obtained from Gibco BRL (Grand Island, NY, USA). Note that all solvents and reagents used in this study were analytical grade.

### Preparation of PTX or Calcein-Loaded FA-TATp-PLs

#### *Preparation of FA-PLs*

FA-PLs were prepared using the thin-film hydration method as described previously (26,27). In brief, FA-OQLCS,

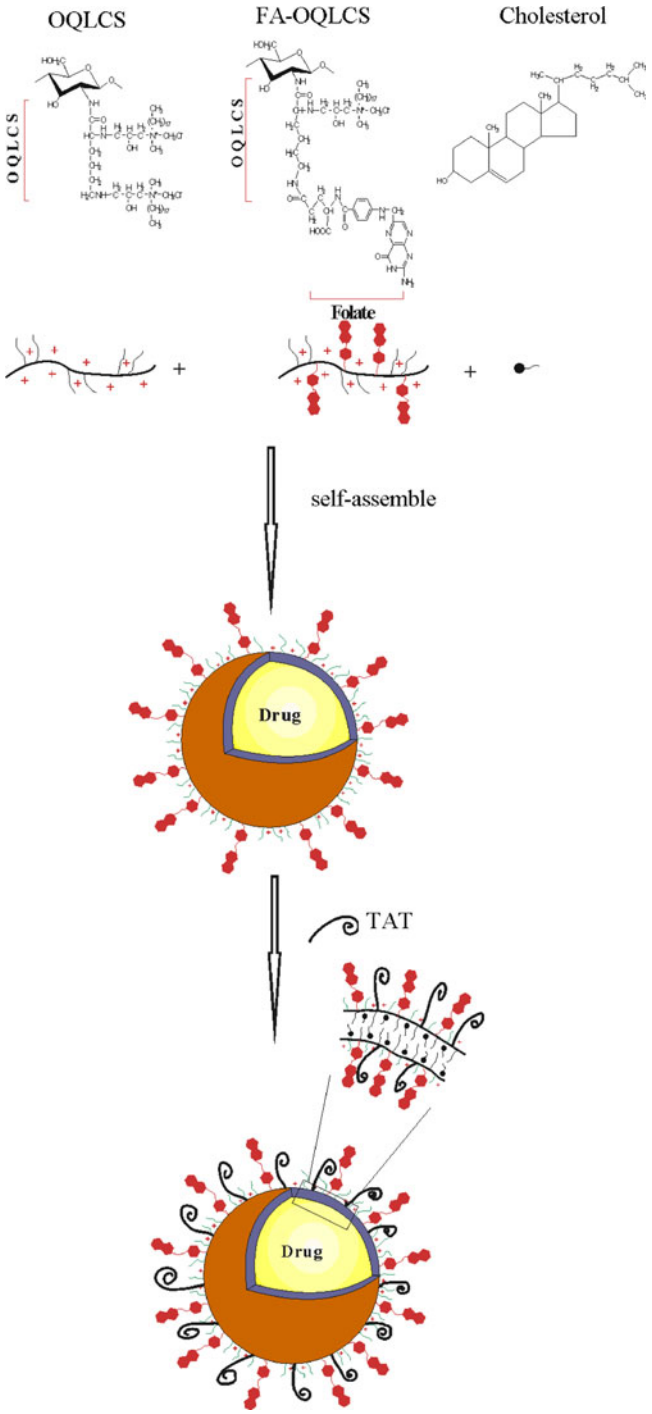


**Fig. 1** Synthesis process of folic-acid-targeted and TAT-peptide-conjugated polymeric liposomes.

OQLCS and cholesterol (w/w/w 1:1:1 total weight 20 mg) were dissolved in chloroform. After chloroform was evaporated with a vacuum rotary evaporator, a thin film of PLs formed, was resuspended in PBS and then freeze-dried. The final FA-PLs were stored in tight containers at 4°C for further experiments.

### *Synthesis of TATp-PLs and FA-TATp-PLs*

TATp-modified PLs and FA-PLs were prepared according to the literature with slight modification (28). TATp was first modified at its N-terminus by Sulfo-LC-SPDP. Briefly, 1 ml TATp (5 mg/ml in PBS, pH 7.4) was mixed with 5-fold molar excess of Sulfo-LC-SPDP, dissolved in DMSO, and reacted at 37°C for 5 h. Sulfo-LC-SPDP-modified TATp was then treated with DTT at 37°C for 2 h to link the free sulfhydryl group to the N-terminus of TATp. To synthesize the final TATp-modified PLs and FA-PLs, 2 ml PLs and FA-PLs solution (5 mg/ml) were mixed with sulfhydryl-TATp (20-fold molar excess of SH-Sulfo-LC-SPDP: PLs or FA-PLs) and reacted at 4°C for 8 h. TATp-PLs and FA-TATp-PLs were purified by Sephadex G25 Column (GE Healthcare, NJ, USA) and then were concentrated and lyophilized. After incubation of Sulfo-LC-SPDP-modified TAT peptide with PLs or FA-PLs solutions, the concentration of the cleavage product, pyridine-2-thione (P2T), was measured and calculated by spectrophotometer (29).

### *PTX or Calcein Encapsulation*

The PTX-loaded PLs, FA-PLs and FA-TATp-PLs were prepared according to a modified procedure (30). In short, 50 mg PLs, FA-PLs or FA-TATp-PLs were dissolved in 5 mL PBS, and then a given amount of PTX in chloroform was slowly transferred via pipetting into the above solutions and stirred in the dark for 24 h. The solutions were lyophilized to remove chloroform. The remaining solids were redispersed into 5 ml of PBS and filtered using Sephadex G25 Column to remove free PTX. The final solutions were freeze-dried and stored under light protection at −20°C until further use. The fluorescent calcein-loaded PLs, FA-PLs and FA-TATp-PLs were prepared in the same manner, except that 0.1% (w/w) calcein was added to the above PLs solutions rather than PTX.

## Characterizations of FA-TATp-PLs and PTX-Loaded FA-TATp-PLs

### *Particle Size, Polydispersity and Zeta Potential*

The particle size, polydispersity and zeta potential of different PTX-loaded FA-TATp-PLs were determined at 25°C by dynamic light scattering (DLS) using a Brookhaven Zetasizer (Brookhaven Instruments Ltd., NY, USA). Three different samples were prepared, measured and averaged.

### *Morphology*

The morphologies of PTX-loaded and unloaded FA-TATp-PLs were observed using transmission electron

microscopy (TEM, JEOL-100CXII, Japan). One drop of the sample solution was deposited onto a carbon-coated copper grid, counterstained with 2% phosphotungstic acid and air-dried at room temperature prior to examination under TEM.

### *Loading Efficiency and Encapsulation Rate*

To determine the drug LE and encapsulation rate (ER), a predetermined aliquot of PTX-loaded FA-TATp-PLs was first eluted through Sephadex G25 Column to remove any free PTX. The drug concentrations in FA-TATp-PLs before and after elution were determined by using high performance liquid chromatography (HPLC). Briefly, 10 μl aliquot were assayed for the PTX concentration under the following experimental conditions: Comatex C18 (150 mm×4.6 mm, 5 μm), mobile phase: methanol: acetonitrile:water (35:40:25,v/v/v), flow rate: 1.0 ml/min, wavelength: 227 nm. The percentage of the drug entrapped in the FA-TATp-PLs was calculated as follows:

LE(%)=(amount of the drug in FA-TATp-PLs / amount of the feeding material and drug)×100%;
ER(%)=(amount of the drug in FA-TATp-PLs / amount of the feeding drug)×100%.

## *In Vitro* PTX Release from PTX-Loaded FA-TATp-PLs and Taxol

The release profiles of PTX from the FA-TATp-PLs in PBS at 37°C were evaluated for 2 weeks by a dialysis method and were compared with that of Taxol®. PTX-loaded FA-TATp-PLs (50 mg) were dispersed in 5 ml of releasing medium (PBS) and were placed into a cellulose membrane dialysis tube (MW cutoff=12,000–14,000). To enhance the solubility of PTX, the dialysis tube was placed into 200 ml of PBS containing 0.1% (v/v) Tween-80 and gently shaken at 37°C in a water bath at 300 rpm. Periodically, 1 ml releasing medium was withdrawn and refilled with the same amount of the fresh medium, and PTX concentrations were determined by RP-HPLC as noted above.

## Cell Culture

The human KB nasopharyngeal epidermal carcinoma cell line overexpressing FR was obtained from American Type Culture Collection (Manassas, VA, USA). The FR-deficient A549 lung adenocarcinoma cell line was purchased from Institute of Basic Medical Science, Chinese Academy of Medical Science (Beijing, China). Both cell lines were cultured continuously as a monolayer at 37°C in a humidified atmosphere containing 5% $CO_2$. Cells were all cultured in FA-deficient RPMI1640 medium supplemented with 1% penicillin, 1% streptomycin, and 10% heat-inactivated fetal bovine serum. The serum contains endogeneous FA at concentrations sufficient for cells to grow (31).

## Cellular Uptake Studies

The cellular uptake of calcein formulations (denoted as calcein-loaded PLs, FA-PLs, TATp-PLs, FA-TATp-PLs) was evaluated in KB and A549 cells by using flow cytometry and confocal laser scanning microscopy (CLSM).

In brief, $5\times10^5$ cells were seeded into 6 cm Petri dish for 24 h before treatments. Cells were allowed to be incubated with various calcein-encapsulated PLs at the lipid concentration of 6 μg/ml using FDRPMI-1640 medium containing 10% HIFBS. After 1 h incubation at 37°C, cells were washed three times with cold PBS to remove unbound liposomes, detached with 0.25% trypsin, centrifuged at 1,000 rpm for 5 min and then suspended in 1 ml of PBS. The suspended cells were directly introduced into a flow cytometer (Beckman Coulter, Foster City, CA, USA) and analyzed under the excitation and emission wavelengths of 488 and 520 nm, respectively. At least 10,000 fluorescent events were recorded for each sample. The autofluorescence of untreated cells was used as controls.

The cellular uptake of calcein formulations (denoted as calcein-loaded PLs, FA-PLs, TATp-PLs and FA-TATp-PLs) was evaluated in KB and A549 cells by using CLSM. For each cell line, $3\times10^3$ cells were seeded onto the 18-mm diameter circle coverslips in 12-well culture plate and incubated for 24 h at 37°C to encourage cell adhesion and spread. Cells were then incubated with calcein-encapsulated PLs at the lipid concentration of 6 μg/ml for 2 h, followed by washing with cold PBS three times. After being fixed with 4% paraformaldehyde in PBS at room temperature for 10 min, cells were treated with 1 ml 0.01% Triton-X-100 for 10 min. Next, cells were washed three times with PBS and incubated at 37°C with 10 μl 2 μg/ml DAPI for 10 min. Finally, coverslips containing cells were mounted onto slides and were observed using a Leica TCS SP5 CLSM (Heidelberg, Germany). The emission wavelength was set at 488 nm for calcein. The images were superimposed using the imaging software to observe colocalization.

## *In Vitro* Cytotoxicity Assay

The cytotoxicity of Taxol®, PTX-loaded PLs, PTX-loaded FA-PLs and PTX-loaded FA-TATp-PLs were assessed by a colorimetric MTT assay. KB and A549 cells were seeded at a density of $5\times10^3$ cells/well in 96-well plates and allowed to adhere for overnight. Cells were treated with PTX concentrations ranging from 0.0001 to 5 μg/ml in free form as well as in liposomal formulations. Cells were subsequently

incubated for 72 h at 37°C, and a total volume of 20 μl of 5 mg/ml MTT solution were added to each well. The plates were further incubated for 4 h at 37°C in the dark. The culture medium was subsequently discarded, and 150 μl of DMSO was added to dissolve the dark-blue formazan crystals. Cell proliferation and viability were quantified spectrophotometrically by measuring the absorbance of the formazan product at the wavelength of 490 nm with a microplate reader (Model 680, Biorad). The data are expressed as the percentages of viable cells compared to the survival of a control group (untreated cells as controls of 100% viability). In addition, the cytotoxicity of PLs, FA-PLs and FA-TATp-PLs without PTX was also assessed against KB and A549 cells in the same manner in the whole range of concentrations examined during the treatment with PTX formulations. The data were expressed as the mean ± standard deviation (SD) of six individual measurements.

### Animals

Four-to-six-week-old severe combined immunodeficiency (SCID) female mice (Vital Laboratory Animal Center, Beijing, China), bred in our specific-pathogen-free facility, were used as animal models. Mice were housed five per cage, exposed to 12-h light-dark cycles, and given free access to sterilized FA-free food (Vital Laboratory Animal Center, Beijing, China) and sterilized water. The animal experiments were performed in accordance with the guidelines for animal experiments and care approved by Tianjin Medical University.

### *In Vivo* Studies

KB cells were injected s.c. ($1\times10^6$ cells/mouse) in the right flank region of SCID mice. Treatments were started when the tumors reached a volume of 100 $mm^3$, which was designated day 0 (about 16 days after inoculation). Tumor-bearing mice were randomly divided into 4 groups ($n=10$). Mice in the treatment groups were injected with PBS, FA-TATp-PLs, Taxol® (10 mg PTX/kg) and PTX-loaded FA-TATp-PLs (10 mg PTX/kg) via tail vein using a 1.0 ml syringe, respectively. The antitumor activity was evaluated in terms of tumor volume size (V) every three days for up to 21 days, as estimated by the following equation: $V=a\times b^2/2$, where a and b are the largest and the smallest diameter of the tumor measured by a vernier caliper.

### Statistical Analysis

Differences of *in vitro* and *in vivo* antitumor activity between Taxol® and PTX-loaded FA-TATp-PLs were examined using one-way ANOVA. Data were presented as the mean ± SD, and all experiments were independently repeated at least three times. *P*-values < 0.05 (two-sided) were considered as statistically significant.

## RESULTS AND DISCUSSION

### Conjugation of FA and TAT to PLs

In our previous work, OQLCS and FA-modified OQLCS were successfully synthesized, and the conjugation of FA with OQLCS was also confirmed through the analysis of $^1$H NMR and FTIR (26). To determine the average number of TAT peptide conjugated on the surface of PLs and FA-PLs, a P2T method was adapted (32,33). By measuring the specific absorption of the released P2T at 343 nm, the estimated amount of TAT peptide attached to PLs and FA-PLs surface was found to be about 0.25 mg per mg of PLs and FA-PLs, which can be changed by controlling the quantity of SPDP and TAT peptide.

### Physicochemical Characterizations

#### *Particle Size and Polydispersity*

The particle size and polydispersity of FA-TATp-PLs and PTX or calcein-loaded FA-TATp-PLs in PBS were determined by DLS. The results are displayed in Table I and Fig. 2. DLS measurements indicated that the FA-TATp-PLs had a mean particle size of 60.5±3.5 nm. There was no significant difference in particle size between PLs and FA-TATp-PLs because folic acid and TAT peptide are both micromolecules. The diameter of calcein-loaded FA-TATp-PLs was 61.2±4.2 nm. The particle size of PTX-loaded FA-TATp-PLs was positively correlated with the increase of loading efficiency of PTX. Particle size is a key parameter determining the cellular uptake of the liposomes. Liposomes with a small particle size (<200 nm) may be prone to minimize the particle uptake in non-targeted cells, including their premature clearance by the mononuclear phagocytic system. PTX or calcein-loaded and unloaded FA-TATp-PLs exhibited a narrow size distribution (polydispersity index ≤0.2).

#### *Surface Morphology*

As evidenced by the representative images showing the external structure of the FA-TATp-PLs and PTX-loaded FA-TATp-PLs, the mean diameters of PTX-loaded and non-loaded FA-TATp-PLs determined by TEM were smaller than the values obtained by DLS (Fig. 2A, B). The diameter obtained from the DLS experiment reflects the hydrodynamic diameter of the liposomes, whereas the diameter observed under TEM shows that of dried liposomes.

**Table I** Physicochemical Characterization of PTX- or Calcein-Loaded FA-TATp-PLs

| Samples | Loading efficiency(%) | Encapsulation efficiency (%) | Particle size (nm) | Polydispersity | Zeta potential |
|---|---|---|---|---|---|
| PLs | 0 | 0 | 60.5 ± 3.5 | 0.18 ± 0.02 | 28.69 ± 0.45 |
| calcein-PLs | 0.1 | 100 | 61.2 ± 4.2 | 0.17 ± 0.02 | 27.94 ± 0.73 |
| PTX 6 wt%-PLs | 5.71 ± 0.12 | 95.11 ± 2.02 | 60.3 ± 5.5 | 0.18 ± 0.02 | 29.23 ± 1.02 |
| PTX 11 wt%-PLs | 9.55 ± 0.31 | 86.83 ± 2.73 | 63.7 ± 4.6 | 0.18 ± 0.01 | 31.33 ± 0.95 |
| PTX 16 wt%-PLs | 10.09 ± 0.71 | 63.03 ± 4.45 | 63.7 ± 6.2 | 0.14 ± 0.01 | 32.43 ± 1.48 |
| PTX 20 wt%-PLs | 8.57 ± 0.54 | 42.85 ± 2.69 | 67.3 ± 4.5 | 0.20 ± 0.02 | 33.04 ± 0.69 |
| PTX 26 wt%-PLs | 7.88 ± 1.42 | 30.29 ± 5.48 | 77.7 ± 7.1 | 0.20 ± 0.01 | 33.67 ± 0.20 |

Therefore, an increase in the liposome size obtained from DLS as compared to that of TEM is probably due to the dehydration and shrinkage of liposomes during drying. Similar difference in size on account of different measurement techniques was also found in the literature (34).

### *Zeta Potential*

Zeta potential is another important factor leading to efficient intracellular trafficking of liposomes (35). As shown in Table I, the zeta potential value of FA-TATp-PLs in PBS was 28.69 ± 0.45 mv, very close to that of PTX- or calcein-loaded FA-TATp-PLs, indicating that the conjugation with PTX or calcein did not greatly alter the zeta potential value of FA-TATp-PLs. Moreover, positive surface charge of liposomes may encourage them to interact with negatively charged cellular surfaces. In addition, our data are also in support of the notion that high surface charge leads to strong repellent interactions among the liposomes in dispersion, thereby resulting in high stability (Fig. 2C).

### *Loading and Encapsulation Efficiency*

To obtain the optimal encapsulation condition, different PTX loading experiments were further conducted. When the feed ratio of PTX to FA-TATp-PLs was increased from 6% to 26% (weight), the encapsulation rate was decreased from 95.11 ± 2.02% to 30.29 ± 5.48% (Table I). This is probably because the feed concentration is much higher than its saturation solubility. Based on these experiments, we chose 11% as the feed ratio of PTX to FA-TATp-PLs in our following experiments except otherwise stated, because it showed a sufficiently high loading amount with a higher encapsulation efficiency (86.83 ± 2.73%).

## *In Vitro* Drug Release

Next, we attempted to quantify and compare the cumulative release of PTX from PTX-loaded FA-TATp-PLs and Taxol® in PBS in 14 days (Fig. 3). In contrast to a significant burst release at the initial stage reported in other literatures (36,37), our FA-TATp-PLs released 40% PTX in the first 2 days and 55% PTX in 5 days, followed by a 25% PTX release in the next 9 days and did not show an evident burst release in the release profile. In addition, almost all the PTX discharged from the Cremophor® EL-based formulation (Taxol®) in 2 days. At the early stages, the fast release of PTX from FA-TATp-PLs may be due to the dissolution and diffusion of drug that was poorly loaded in the core of FA-TATp-PLs, while the slow and continuous release may result

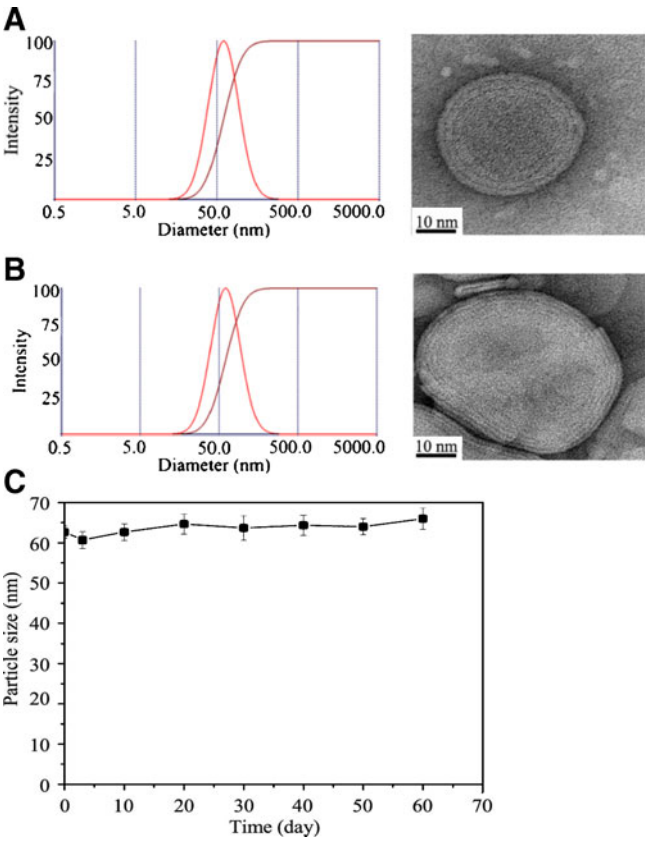


**Fig. 2** Particle sizes and morphological shapes of FA-TATp-PLs (**A**) and PTX-loaded FA-TATp-PLs (**B**). The diameters and morphological shapes of FA-TATp-PLs and PTX-loaded FA-TATp-PLs were determined by DLS and TEM at the lipid concentration of 1 mg/ml. Scale bar: 10 nm. (**C**) The change in the size of FA-TATp-PLs through 2-month observation.

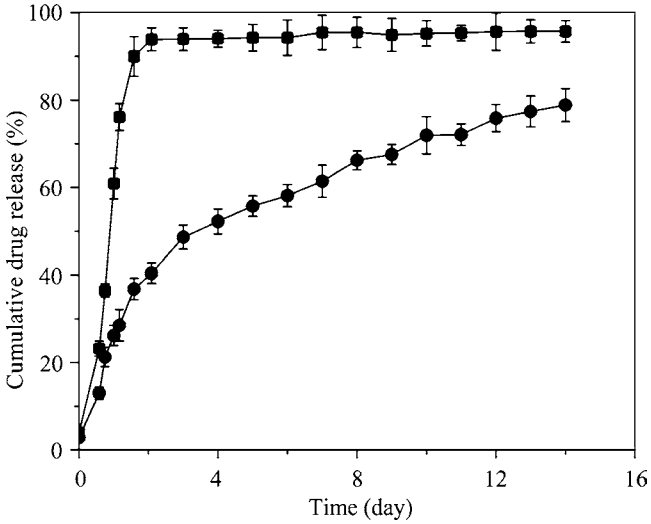


**Fig. 3** *In vitro* release profile of paclitaxel from Taxol® (■) and PTX-loaded FA-TATp-PLs (●) in PBS (PH 7.4, 37°C) for 2 weeks. Data are expressed as the mean ± SD ($n = 3$).

from the erosion and degradation of the FA-TATp-PLs (38,39). This sustained release profile has been proposed in drug delivery system that could prolong the duration of therapeutic concentration of PTX. Moreover, our data from the HPLC analyses revealed that the released PTX from FA-TATp-PLs had the same retention time as that from Taxol®, indicating that the chemical structure of PTX in the FA-TATp-PLs was not changed.

## Cellular Uptake of Calcein Formulations

It is clear that the cellular uptake efficiency of drug-loaded PLs affects the therapeutic effects. Liposomes labeled with fluorescent dyes are frequently used to study cellular uptake. In addition, calcein is a common model drug for liposomes to study the cellular uptake behavior.

We studied the cellular uptake efficiency of various calcein-loaded PLs in FR-positive KB cells by using a series of flow cytometric analyses (Fig. 4A). FA-PLs, TATp-PLs and especially FA-TATp-PLs had a higher cellular uptake than that of PLs. There was no significant fluorescence shift between FA-PLs and TATp-PLs. For the sake of comparison, we chose FR-deficient A549 cells as negative controls. As shown in Fig. 4B, the fluorescence histogram of cells incubated with calcein-loaded PLs was similar to that of cells incubated with calcein-loaded FA-PLs, while a distinguishable right shift was observed in the calcein-loaded TATp-PLs and FA-TATp-PLs, suggesting an increased cellular uptake.

To further evaluate the role of FA ligand and TAT peptide and their potential interaction in cellular uptake of calcein formulations, the cellular uptake of various calcein-loaded PLs was quantified by measuring the mean fluorescence intensity per cell. Differing from the observations seen in A549 cells (TATp-PLs *vs* PLs: 2.63-fold; FA-TATp-PLs *vs* PLs: 3.38-fold), the mean fluorescence intensities of TATp-PLs and FA-TATp-PLs were significantly increased by 6.67- and 24.27-fold than PLs in KB cells.

The cellular uptake of calcein formulations was visualized in KB and A549 cells by using CLSM (Figs. 5 and 6). To further precisely determine the cellular distribution, we performed double fluorescence-labeling experiments and visualized green fluorescence from calcein and blue fluorescence from DAPI selectively labeling the nucleus. No fluorescence was detectable in cells incubated with calcein, indicating that calcein is membrane-impermeable fluorophore (Figs. 5A and 6A). As described in Fig. 5, intense calcein fluorescence from calcein-loaded FA-PLs in the cytoplasm was observed in FR-positive KB cells in comparison with negligible fluorescence from PLs without targeting effect, suggesting that FA-conjugated PLs were taken up more efficiently into KB cells (Fig. 5C, B). When compared to that of FA-PLs, the confocal images of the TATp-PLs showed similar fluorescence intensities in the cytoplasm (Fig. 5D). Moreover, cells treated with FA-TATp-PLs showed not only strong fluorescence in cytoplasm, but also internalization of the particles and their accumulation in cell nucleus. These results indicate that the presence of FA and TAT peptide on the PLs' surface could facilitate the transport of PLs into the nucleus (Fig. 5E).

Subsequently, we tested whether calcein-loaded PLs could deliver calcein into A549 cells without FR (Fig. 6). Our results revealed that the FA-targeted and untargeted calcein-PLs had minimal uptake (Fig. 6B, C). This is expected since the internalization of FA-targeted PLs was mediated through FR-dependent targeting (40). Cells treated with TATp-PLs and FA-TATp-PLs showed intense green fluorescence due to the cell-penetrating activity of TAT peptide, and calcein accumulated mostly in the perinuclear region (Fig. 6D, E). Nevertheless, loss of the targeting effect of FA moiety may greatly affect the ability of FA-TATp-PLs to enter A549 cells as compared to that in KB cells (Figs. 5E and 6E).

Two major conclusions can be made from the above results. First, the fluorescence of calcein from TATp-PLs was strong, irrespective of the expression of FR in cancer cells. However, the transmembrane ability of TAT peptide in KB cells and A549 cells was different. TATp-modified PLs enter the interior of KB cells more easily when compared to that of A549 cells. Second, FA-TATp-PLs unifying the targeting effect of FA and the transmembrane ability of TAT peptide were taken up more efficiently into cancer cells, especially into the FR-positive cells.

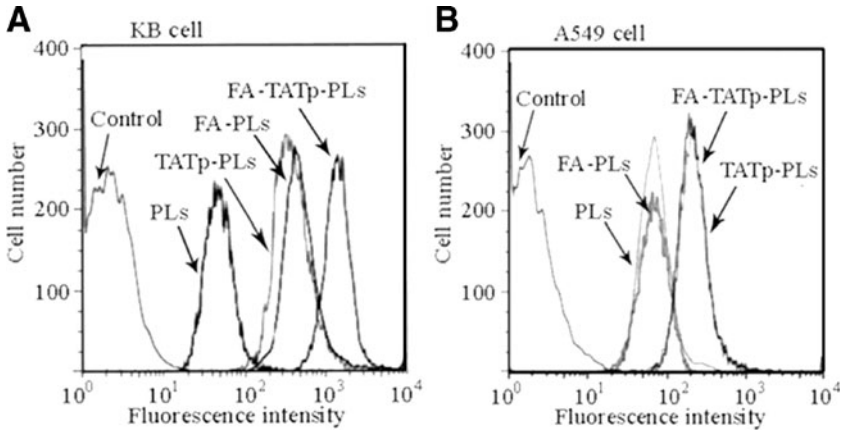


**Fig. 4** Cellular uptake of various PLs encapsulating calcein in KB (**A**) or A549 (**B**) cells by flow cytometric analyses after 1 h incubation. Control indicates the autofluorescence of untreated cells.

### *In Vitro* Cytotoxicity Assay

In FR-positive KB cells, the cytotoxicity of different PTX formulations was basically in the following order: FA-TATp-PLs >FA-PLs >Taxol® >PLs (Fig. 7A, Table II). The order of antitumor effects was in accordance with that of the cellular uptake assays. In addition, the cell killing effect of PTX formulations was concentration-dependent. The MTT analyses demonstrated that PTX-PLs were less cytotoxic than Taxol®, probably owing to the poor cellular uptake of PLs. In addition, the cytotoxicity of the paclitaxel-loaded liposomes was dominated by the actual intracellular drug concentration. Interestingly, the modification of FA and TAT peptide could evidently reverse the trend: PTX-FA-PLs and PTX-FA-TATp-PLs had higher drug efficacies than Taxol® (Fig. 7A). Particularly, PTX-FA-TATp-PLs were even more effective, indicating that FA surface modification was not compromised by TAT peptide conjugation, but actually facilitated a more efficient delivery of PTX into FR-positive KB cells. Importantly, PLs, FA-PLs and FA-TATp-PLs without PTX did not have any apparent effect on the proliferation of KB and A549 cells in the whole range of concentrations examined during the treatment with PTX formulations (data not shown), confirming that anticancer activity was due to drug delivery, rather than the carrier system.

In contrast, there was no significant difference of *in vitro* cytotoxicity among Taxol®, PTX-PLs and PTX-FA-PLs in the FR-negative A549 cells at the most of concentrations tested (Fig. 7B, Table II). However, we did notice that PTX-loaded FA-TATp-PLs showed higher tumor suppression efficiency than other PTX formulations except at the concentration of 0.001 μg/ml, suggesting that TAT peptide still played a key role in facilitating the cellular uptake of PLs in A549 cells without FR.

In summary, our *in vitro* cytotoxicity demonstrated that TAT peptide conjugation and active targeting of FA ligand could function simultaneously to increase the cytotoxicity of paclitaxel in FR-upregulated KB cells as well as in FR-deficient A549 cells.

### *In Vivo* Antitumor Activity

As described above, both the cellular uptake assays and *in vitro* cytotoxicity studies demonstrated the targeting effect of FA moiety and the transmembrane ability of TAT peptide and also showed that PTX-loaded FA-TATp-PLs were more cytotoxic than Taxol®. As a result, we decided to further confirm whether PTX-loaded FA-TATp-PLs had a higher antitumor activity *in vivo* as compared to Taxol®.

The antitumor efficacy of Taxol® and PTX-loaded FA-TATp-PLs was evaluated in mice bearing nasopharyngeal tumors. The tumor growth rate in mice treated with FA-TATp-PLs without PTX was very similar to that of tumors in PBS-treated mice (Fig. 8), indicating that the FA-TATp-PLs had no effect on tumor growth. Conversely, significant antitumor effect of Taxol® and PTX-loaded FA-TATp-PLs was observed. By 21 days after injection, the average tumor volume in Taxol®-treated mice and PTX-loaded FA-TATp-PLs-treated mice had increased relatively slowly and attained about 692 and 431 $mm^3$, while the average tumor volume in PBS and FA-TATp-PLs-treated mice was 1,255 and 1,228 $mm^3$. Especially, PTX-loaded FA-TATp-PLs showed a significantly higher antitumor efficacy than did free PTX (Fig. 8).

Based on the measurement of tumor volume, it is possible to conclude that PTX-loaded FA-TATp-PLs showed significant antitumor efficacy. In order to deliver

**Fig. 5** Confocal laser scanning microscopic images of KB cells after 2 h incubation with calcein-loaded (**B**) PLs, (**C**) FA-PLs, (**D**) TATp-PLs, (**E**) FA-TATp-PLs at a concentration of 6 μg/ml. Cells treated with calcein (**A**) were used as control. The left images were obtained from FITC channel (green), which shows the fluorescence of calcein; the middle were from DAPI channel (blue), which shows the nuclei staining; the right are merged pictures from previous two images. Scale bar: 25 μm.

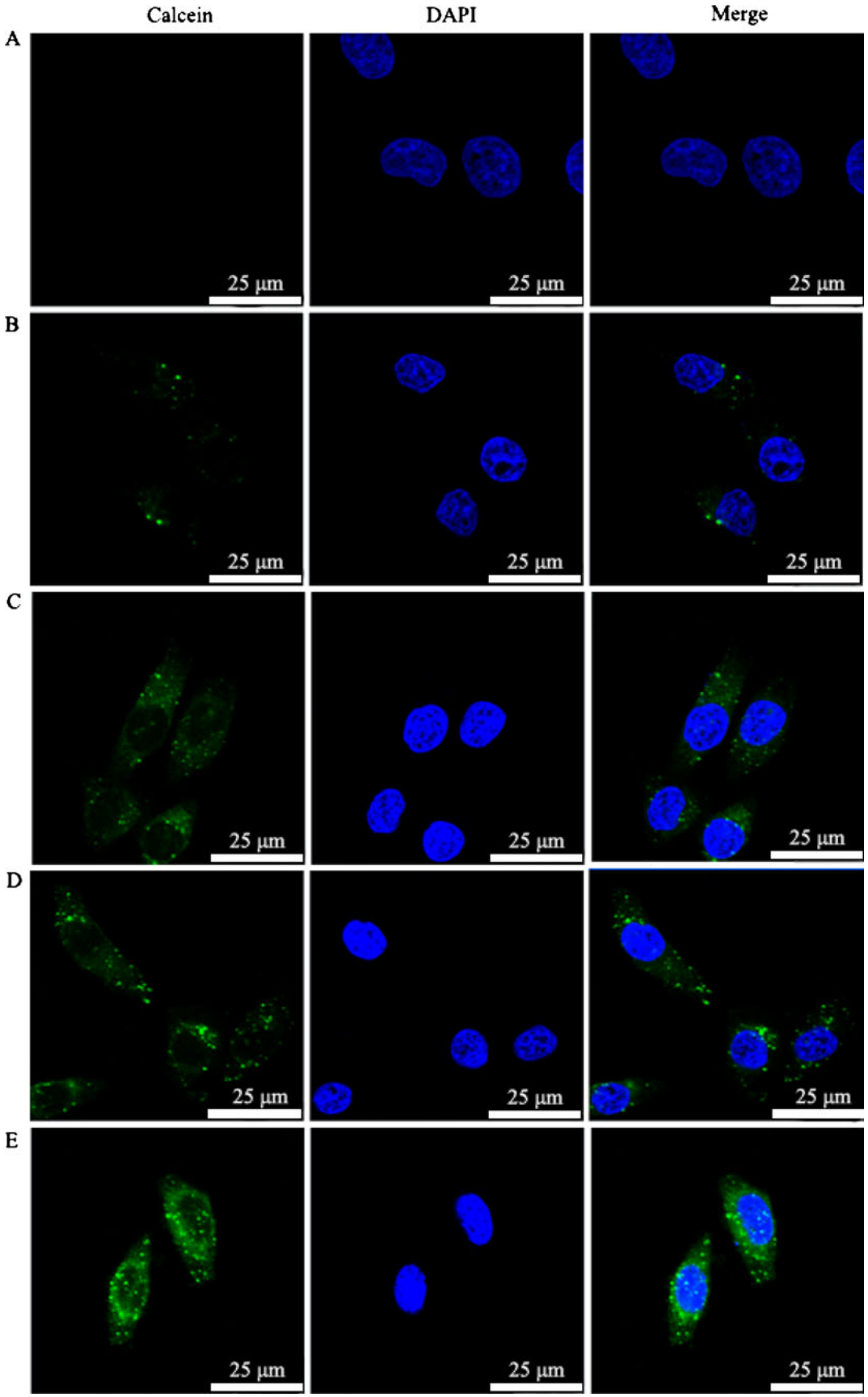
Calcein
DAPI
Merge
A
B
C
D
E
25 μm

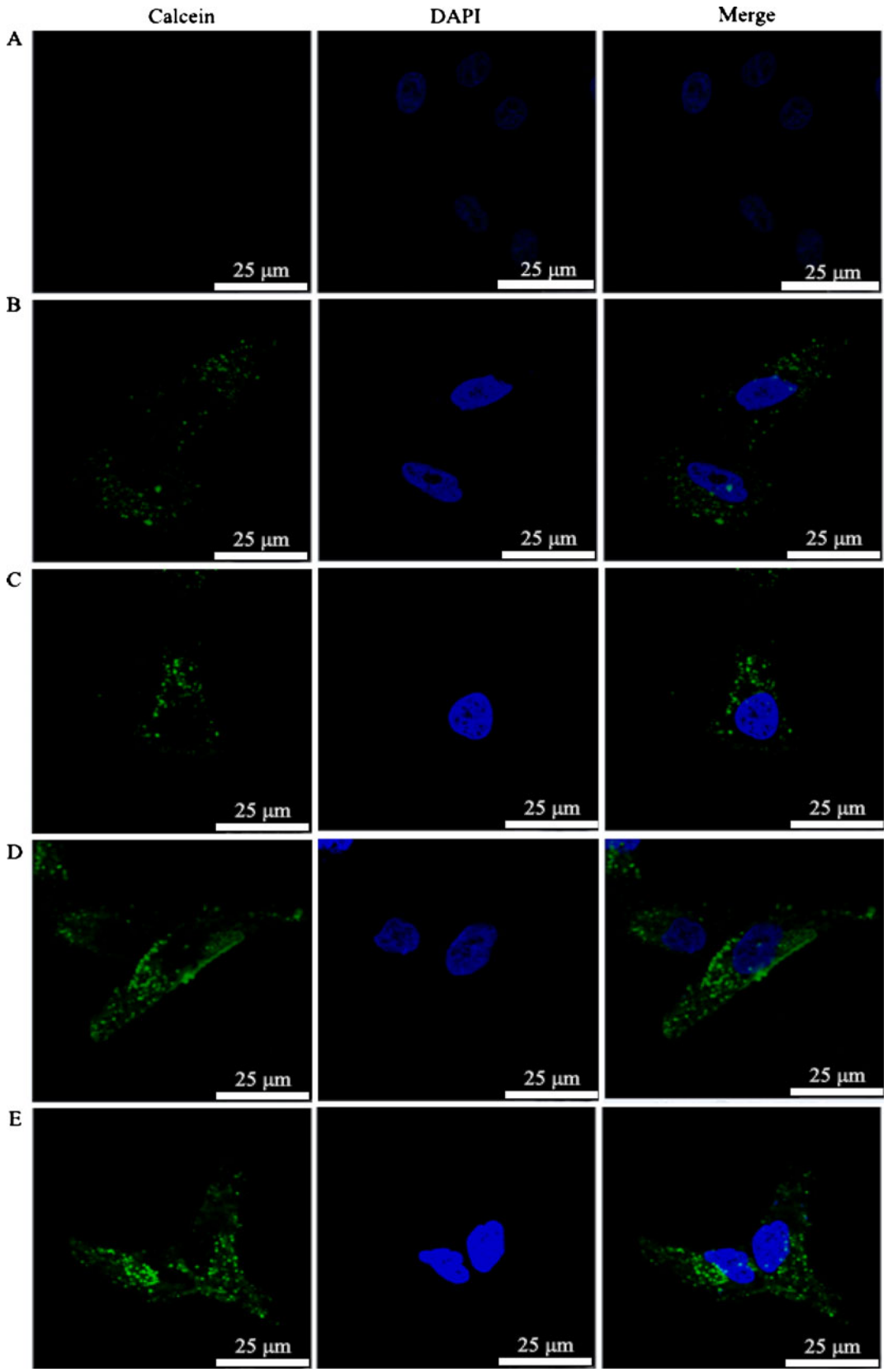


**Fig. 6** Confocal laser scanning microscopic images of A549 cells after 2 h incubation with calcein-loaded (**B**) PLs, (**C**) FA-PLs, (**D**) TATp-PLs, (**E**) FA-TATp-PLs at a concentration of 6 $\mu$g/ml. Cells treated with calcein (**A**) were used as control. The left images were obtained from FITC channel (*green*), which shows the fluorescence of calcein; the middle were from DAPI channel (*blue*), which shows the nuclei staining; the right are merged pictures from previous two images. Scale bar: 25 $\mu$m.

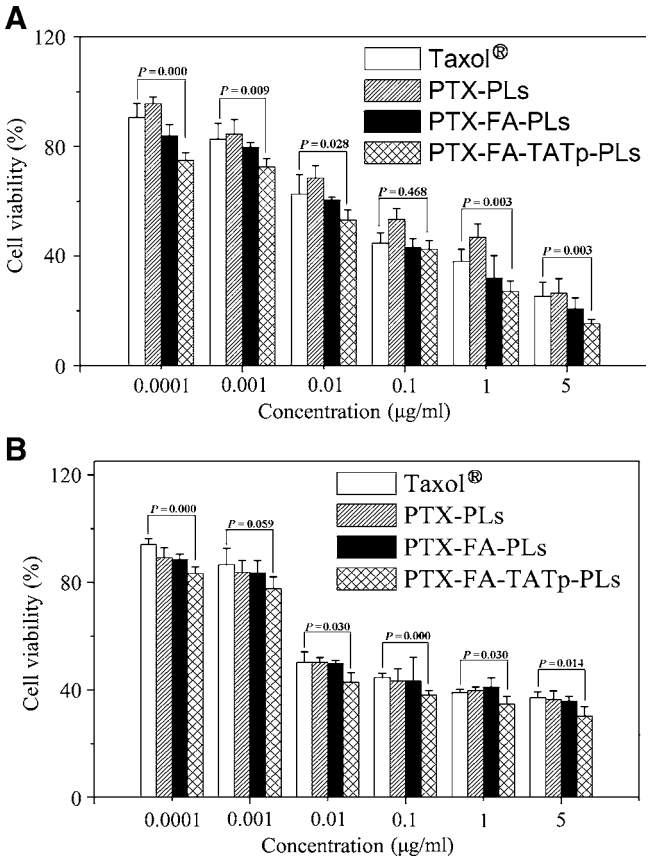


**Fig. 7** Cell viability of (**A**) KB cells and (**B**) A549 cells treated with Taxol®, PTX-PLs, PTX-FA-PLs and PTX-FA-TATp-PLs after 72 h at the concentrations ranging from 0.0001 μg/ml to 5 μg/ml. Data are presented as the mean ± SD compared to the controls. $n = 6$. *P*-values < 0.05 were considered as statistically significant.

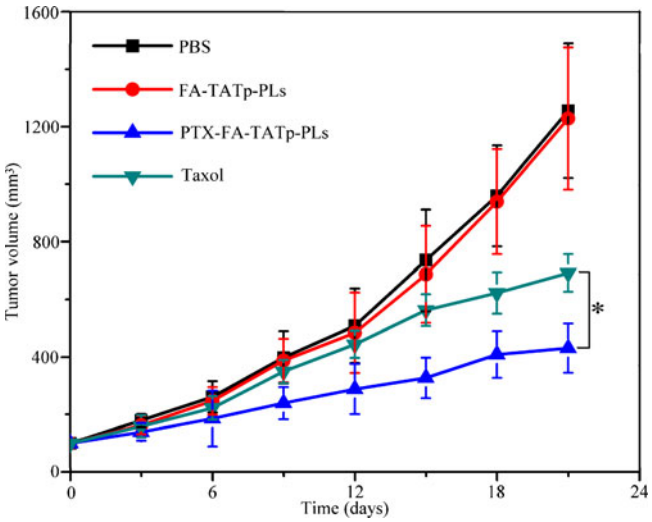


**Fig. 8** *In vivo* antitumor effect of PBS, FA-TATp-PLs without paclitaxel, Taxol® and paclitaxel-loaded FA-TATp-PLs at the doses of 10 mg/kg in SCID mice bearing KB nasopharyngeal cancer (*$P < 0.05$; compared with control; $n = 10$).

drugs into cancer cells, the targeting specificity of FA and the high delivery efficiency of TAT peptide are rather crucial for the drug delivery system. The mechanism of FA-PLs transporting folate-linked cargos into FR-overexpressing KB cells is through a process called receptor-mediated endocytosis (40). Although TAT peptide has shown the potential usefulness of delivering drugs to treat cancers, the concrete mechanism remains unknown. Recent data indicate that TAT-mediated intracellular delivery of nanoparticles occurs through energy-dependent macropinocytosis, with subsequent enhanced escape from endosomes into the cytoplasm (41). Traversing cellular membranes represents a major barrier for the efficient delivery of macromolecules into cells, and therefore TAT peptide, whatever their mechanism of action, could serve to transport various drug-loaded carrier systems into cancer cells *in vitro* and *in vivo*. Our study created the possibility of a single drug delivery system possessing both the targeting effect and the transmembrane ability. Such a dual-function strategy is quite unique and holds the promise towards its implication into targeted anticancer therapeutics.

## CONCLUSIONS

In conclusion, we successfully developed a novel drug delivery system which possesses targeting, transmembrane, and drug sustained-release properties. Our data showed that 80% PTX released from FA-TATp-PLs in 2 weeks and FA-TATp-PLs exhibited more efficient endocytosis ability in both FR-overexpressing KB cells and in FR-deficient A549 cells than PLs. The antitumor activities were also significantly enhanced by encapsulating PTX in FA-TATp-PLs both *in vitro* and *in vivo* in comparison with that of Taxol®. Our findings suggest for the first time that PTX-loaded FA-TATp-PLs may act as a promising model for future tumor cancer therapy, especially for tumors overexpressing FR.

**Table II** The IC 50 Values of PTX Formulations After 72 h Incubation with KB and A549 Cells

| | Taxol (μg/ml) | PTX-PLs (μg/ml) | PTX-FA-PLs (μg/ml) | PTX-FA-TATp-PLs (μg/ml) |
|---|---|---|---|---|
| KB cells | $(1.24 \pm 0.27) \times 10^{-1}$ | $(2.07 \pm 0.48) \times 10^{-1}$ | $(4.46 \pm 0.88) \times 10^{-2}$ | $(1.33 \pm 0.37) \times 10^{-2}$ |
| A549 cells | $(2.20 \pm 0.35) \times 10^{-1}$ | $(1.41 \pm 0.12) \times 10^{-1}$ | $(1.20 \pm 0.18) \times 10^{-1}$ | $(3.75 \pm 1.22) \times 10^{-2}$ |

## ACKNOWLEDGMENTS

The study was supported by the National High Technology Development Project (the "863" project, Grant No. 2007AA021802, No. 2007AA021808, No. 2006AA02A249).

## REFERENCES

1. Chua DT, Sham JS, Au GK. A phase II study of docetaxel and cisplatin as first-line chemotherapy in patients with metastatic nasopharyngeal carcinoma. Oral Oncol. 2005;41:589–95.
2. McCarthy JS, Tannock IF, Degendorfer P, Panzarella T, Furlan M, Siu LL. A phase II trial of docetaxel and cisplatin in patients with recurrent or metastatic nasopharyngeal carcinoma. Oral Oncol. 2002;38:686–90.
3. Horwitz SB. Taxol (paclitaxel): mechanisms of action. Ann Oncol. 1994;5 Suppl 6:S3–6.
4. Liebmann J, Cook JA, Mitchell JB. Cremophor EL, solvent for paclitaxel, and toxicity. Lancet. 1993;342:1428.
5. Schmitt-Sody M, Strieth S, Krasnici S, Sauer B, Schulze B, Teifel M, *et al.* Neovascular targeting therapy: paclitaxel encapsulated in cationic liposomes improves antitumoral efficacy. Clin Cancer Res. 2003;9:2335–41.
6. Sutton D, Nasongkla N, Blanco E, Gao J. Functionalized micellar systems for cancer targeted drug delivery. Pharm Res. 2007;24:1029–46.
7. Fonseca C, Simoes S, Gaspar R. Paclitaxel-loaded PLGA nanoparticles: preparation, physicochemical characterization and *in vitro* anti-tumoral activity. J Control Release. 2002;83:273–86.
8. Gupte A, Ciftci K. Formulation and characterization of Paclitaxel, 5-FU and Paclitaxel + 5-FU microspheres. Int J Pharm. 2004;276:93–106.
9. Mitra A, Lin S. Effect of surfactant on fabrication and characterization of paclitaxel-loaded polybutylcyanoacrylate nanoparticulate delivery systems. J Pharm Pharmacol. 2003;55:895–902.
10. Kukowska-Latallo JF, Candido KA, Cao Z, Nigavekar SS, Majoros IJ, Thomas TP, *et al.* Nanoparticle targeting of anticancer drug improves therapeutic response in animal model of human epithelial cancer. Cancer Res. 2005;65:5317–24.
11. Obara K, Ishihara M, Ozeki Y, Ishizuka T, Hayashi T, Nakamura S, *et al.* Controlled release of paclitaxel from photocrosslinked chitosan hydrogels and its subsequent effect on subcutaneous tumor growth in mice. J Control Release. 2005;110:79–89.
12. Ruel-Gariepy E, Shive M, Bichara A, Berrada M, Le Garrec D, Chenite A, *et al.* A thermosensitive chitosan-based hydrogel for the local delivery of paclitaxel. Eur J Pharm Biopharm. 2004;57:53–63.
13. Zentner GM, Rathi R, Shih C, McRea JC, Seo MH, Oh H, *et al.* Biodegradable block copolymers for delivery of proteins and water-insoluble drugs. J Control Release. 2001;72:203–15.
14. Debbage P. Targeted drugs and nanomedicine: present and future. Curr Pharm Des. 2009;15:153–72.
15. Prato M, Kostarelos K, Bianco A. Functionalized carbon nanotubes in drug design and discovery. Acc Chem Res. 2008;41:60–8.
16. Wang X, Yang L, Chen ZG, Shin DM. Application of nanotechnology in cancer therapy and imaging. CA Cancer J Clin. 2008;58:97–110.
17. Ross JF, Chaudhuri PK, Ratnam M. Differential regulation of folate receptor isoforms in normal and malignant tissues *in vivo* and in established cell lines. Physiologic and clinical implications. Cancer. 1994;73:2432–43.
18. Campbell IG, Jones TA, Foulkes WD, Trowsdale J. Folate-binding protein is a marker for ovarian cancer. Cancer Res. 1991;51:5329–38.
19. Weitman SD, Weinberg AG, Coney LR, Zurawski VR, Jennings DS, Kamen BA. Cellular localization of the folate receptor: potential role in drug toxicity and folate homeostasis. Cancer Res. 1992;52:6708–11.
20. Weitman SD, Lark RH, Coney LR, Fort DW, Frasca V, Zurawski Jr VR, *et al.* Distribution of the folate receptor GP38 in normal and malignant cell lines and tissues. Cancer Res. 1992;52:3396–401.
21. Asoh S, Ohta S. PTD-mediated delivery of anti-cell death proteins/peptides and therapeutic enzymes. Adv Drug Deliv Rev. 2008;60:499–516.
22. Chauhan A, Tikoo A, Kapur AK, Singh M. The taming of the cell penetrating domain of the HIV Tat: myths and realities. J Control Release. 2007;117:148–62.
23. Dietz GP, Bahr M. Delivery of bioactive molecules into the cell: the Trojan horse approach. Mol Cell Neurosci. 2004;27:85–131.
24. Schwarze SR, Ho A, Vocero-Akbani A, Dowdy SF. *In vivo* protein transduction: delivery of a biologically active protein into the mouse. Science. 1999;285:1569–72.
25. Vives E. Present and future of cell-penetrating peptide mediated delivery systems: "is the Trojan horse too wild to go only to Troy?". J Control Release. 2005;109:77–85.
26. Wang H, Zhao P, Liang X, Gong X, Song T, Niu R, *et al.* Folate-PEG coated cationic modified chitosan–cholesterol liposomes for tumor-targeted drug delivery. Biomaterials. 2010;31:4129–38.
27. Liang XF, Wang HJ, Luo H, Tian H, Zhang BB, Hao LJ, *et al.* Characterization of novel multifunctional cationic polymeric liposomes formed from octadecyl quaternized carboxymethyl chitosan/cholesterol and drug encapsulation. Langmuir. 2008;24:7147–53.
28. Moon C, Kwon YM, Lee WK, Park YJ, Yang VC. *In vitro* assessment of a novel polyrotaxane-based drug delivery system integrated with a cell-penetrating peptide. J Control Release. 2007;124:43–50.
29. Josephson L, Tung CH, Moore A, Weissleder R. High-efficiency intracellular magnetic labeling with novel superparamagnetic-Tat peptide conjugates. Bioconjug Chem. 1999;10:186–91.
30. Lin JJ, Chen JS, Huang SJ, Ko JH, Wang YM, Chen TL, *et al.* Folic acid-Pluronic F127 magnetic nanoparticle clusters for combined targeting, diagnosis, and therapy applications. Biomaterials. 2009;30:5114–24.
31. Leamon CP, Low PS. Delivery of macromolecules into living cells: a method that exploits folate receptor endocytosis. Proc Natl Acad Sci USA. 1991;88:5572–6.
32. Zhao M, Kircher MF, Josephson L, Weissleder R. Differential conjugation of tat peptide to superparamagnetic nanoparticles and its effect on cellular uptake. Bioconjug Chem. 2002;13:840–4.
33. Lewin M, Carlesso N, Tung CH, Tang XW, Cory D, Scadden DT, *et al.* Tat peptide-derivatized magnetic nanoparticles allow *in vivo* tracking and recovery of progenitor cells. Nat Biotechnol. 2000;18:410–4.
34. Morita T, Horikiri Y, Suzuki T, Yoshino H. Preparation of gelatin microparticles by co-lyophilization with poly(ethylene glycol): characterization and application to entrapment into biodegradable microspheres. Int J Pharm. 2001;219:127–37.
35. Park MR, Han KO, Han IK, Cho MH, Nah JW, Choi YJ, *et al.* Degradable polyethylenimine-alt-poly(ethylene glycol) copolymers as novel gene carriers. J Control Release. 2005;105:367–80.
36. Kim JH, Kim YS, Park K, Lee S, Nam HY, Min KH, *et al.* Antitumor efficacy of cisplatin-loaded glycol chitosan nanoparticles in tumor-bearing mice. J Control Release. 2008;127:41–9.
37. Min KH, Park K, Kim YS, Bae SM, Lee S, Jo HG, *et al.* Hydrophobically modified glycol chitosan nanoparticles-

encapsulated camptothecin enhance the drug stability and tumor targeting in cancer therapy. J Control Release. 2008;127:208–18.
38. Xu Z, Chen L, Gu W, Gao Y, Lin L, Zhang Z, *et al.* The performance of docetaxel-loaded solid lipid nanoparticles targeted to hepatocellular carcinoma. Biomaterials. 2009;30:226–32.
39. Danhier F, Lecouturier N, Vroman B, Jerome C, Marchand-Brynaert J, Feron O, *et al.* Paclitaxel-loaded PEGylated PLGA-based nanoparticles: *in vitro* and *in vivo* evaluation. J Control Release. 2009;133:11–7.
40. Kamen BA, Capdevila A. Receptor-mediated folate accumulation is regulated by the cellular folate content. Proc Natl Acad Sci. 1986.
41. Wadia JS, Stan RV, Dowdy SF. Transducible TAT-HA fusogenic peptide enhances escape of TAT-fusion proteins after lipid raft macropinocytosis. Nat Med. 2004;10:310–5.